IEEE Access
Multidisciplinary | Rapid Review | Open Access Journal

Received July 15, 2019, accepted July 26, 2019, date of publication August 6, 2019, date of current version September 9, 2019.

Digital Object Identifier 10.1109/ACCESS.2019.2933585

Design of a Low-SLL SIW Slot Array Antenna With a Large Declination in *Ka*-Band

CHENGWEI ZHAO, XIAOPING LI, CHAO SUN, HE HUANG, AND YANMING LIU

Key Laboratory of Information and Structure Efficiency in Extreme Environment, Ministry of Education of China, School of Aerospace Science and Technology, Xidian University, Xi'an 710071, China

Corresponding author: Chengwei Zhao (zhaochengwei@126.com)

This work was supported in part by the Chinese National Natural Science Foundation under Grant 61627901 and Grant 61801343.

ABSTRACT A small-size large-declination longitudinal slot array antenna based on substrate integrated waveguide (SIW) technology was proposed. Compared with the conventional SIW slot array, the proposed antenna achieves a larger declination and a lower SLL. The antenna is mainly composed of three parts, a dielectric substrate, a coaxial port, and a matched load. The antenna contains 13 radiation slots, and the adjacent slot spacing is greater than half of the waveguide wavelength, so the main beam is biased towards the load. To achieve low sidelobe levels (SLL), the amplitude distribution of the 13 slots is based on Taylor synthesis of SLL $= -25$ dB. The antenna was processed and measured. From the measured results, the antenna achieved a beam declination of 26° and a SLL below -20 dB from 35.2 to 35.8 GHz. With the same number of slots, the length of the slot array of the SIW structure is only 44.8% of the length of the standard metal hollow waveguide. Based on the performance achieved, the SIW slot antenna is an excellent candidate for carrier conformal and large declination applications.

INDEX TERMS Substrate integrated waveguide (SIW), traveling-wave array, low sidelobe levels (SLL), main beam declination, *Ka*-band.

I. INTRODUCTION

In projectile communication, the antenna is required to conform to the external surface. At the same time, it is desirable that the antenna main beam has a declination toward the axial direction of the projectile, thereby facilitating the transmission and reception of signals in a desired angle [1]. Therefore, the traveling-wave slot antenna is a suitable candidate. The travelling-wave slot antenna with the frequency-controlled scanning beams and high directivity is a kind of leaky wave antenna. The slot antenna has the advantages of low profile, low or even ultra low SLL, high gain, high radiation efficiency, high power capacity, and easy control of the pattern [2]–[4].

Generally, slot antennas are generally classified into two types: standing-wave arrays and traveling-wave arrays [2]. In the standing-wave arrays, the adjacent slot spacing is $\lambda_g/2$, and the waveguide is shorted at $\lambda_g/4$ (or $3\lambda_g/4$) after the last slot, where λ_g is the wavelength in the waveguide. This structure has high radiation efficiency and the radiation pattern is strictly broadside, but the impedance bandwidth is narrow. For traveling-wave arrays, slots are equally spaced not equal to $\lambda_g/2$ (greater than or less than $\lambda_g/2$), and the waveguide is terminated by a matched load. The main beam of this structure has a declination and the declination varies with frequency. When the slot spacing is less than $\lambda_g/2$, the beam is biased toward the feeding port, and when the spacing is greater than $\lambda_g/2$, the beam is biased toward the load end. The advantages of this configuration are as follows: a) the main beam declination can be achieved, b) the pattern is easy to control, c) a wider impedance and SLL bandwidth compared to standing-wave arrays, although a few power is dissipated by the load.

In the past few years, the waveguide longitudinal slot arrays have been verified by theoretical research, numerical calculations and experimental methods. With Elliott's design procedure, the SLL of a slot array can be accurately synthesized and patterned [3]. The internal mutual coupling and external mutual coupling are considered, and the iterative calculation formula is used to accurately determine the slot parameters for the desired aperture distribution and the input matching. In [5], a method of analyzing the longitudinal slot planar antenna by the full-wave analysis is presented.

The associate editor coordinating the review of this manuscript and approving it for publication was Lu Guo.

The above description of slot antennas is based on conventional metallic waveguides. Recently, the planar waveguide structure, known as the substrate integrated waveguide (SIW), has been investigated [6]–[8]. The SIW structure is used in a variety of frequencies and applications [9]–[20]. The transmission performances of the SIW are very similar to those of a metallic rectangular waveguide. SIW features low profile, convenient processing and easy integration with RF circuits. Therefore, the longitudinal slot array of the SIW structure has a distinct advantage. In [16], a compact single-layer substrate integrated waveguide monopulse slot antenna array is presented. The slot array is in the form of a standing wave array and implements a sum pattern and a difference pattern. In [21], the Method of Least Squares (MLS) was used to develop an optimum design procedure for the traveling-wave SIW slot array antenna. Xu *et al.* [22] showed a 16×16 SIW longitudinal slot array antenna by performing full-wave electromagnetic simulation method. The general SIW slot array antennas are either standing-wave arrays or traveling-wave arrays with a small declination (declination angle $<10°$) [14]–[19], [22]. And when the number of gaps is small (N<15), SLL is poor (SLL> -15 dB) [16]–[18]. Therefore, the design of a large declination, low-SLL SIW slot antenna is very necessary.

In this paper, a small-sized, low-SLL large-declination longitudinal slot array with a SIW structure is proposed. The slot array includes 13 radiation slots. According to the antenna installation requirements, the main beam needs to be biased toward the load, so the slot spacing is greater than $\lambda_g/2$. The slot antenna design is combined with theoretical calculation and software simulation. The power distribution of each slot is adopted with Taylor synthesis of SLL $= -25$ dB, and good performance of SLL < -20 dB is achieved from the measured results.

II. ANTENNA DESIGN

The geometry of the proposed traveling-wave SIW slot array antenna is illustrated in Fig. 1 (a).

Basically, the antenna consists of three parts, a substrate, a coaxial port, and a matched load. There are two rows of metalized vias on both sides of the substrate and 13 radiation slots. The design of the antenna is divided into three parts. Section A is the design of the SIW, Section B is the design of the slot antenna, and Section C is the design of the coaxial to SIW conversion.

A. SIW DESIGN

The SIW is similar to a metal waveguide filled with a dielectric substrate and the structure is shown in Fig. 1 (b). Where d is the diameter of the metallized via, p is the center spacing of adjacent vias, a is the width of the SIW, and b is the height of the dielectric substrate. In order to ensure that the performance of SIW is equivalent to a metal rectangular waveguide, d and p must meet certain design specifications [6],

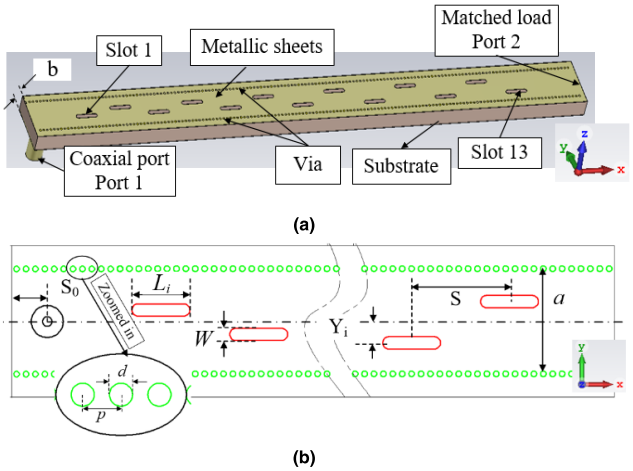

FIGURE 1. Configuration of the proposed antenna. (a) 3-D view. (b) Top view.

the specific requirements are as follows:

$$p < 0.25\lambda_c \tag{1}$$

$$1.2d < p < 2d \tag{2}$$

where λ_c is the cutoff wavelength of the TE_{10} mode. Similar to metallic waveguide transmission, the operating frequency is between the TE_{10} and TE_{20} modes for single mode transmission (TE_{10} mode only). The SIW dielectric substrate was selected as Rogers 5880 with a dielectric constant ε_r of 2.2 and a loss tangent of 0.0009. The center frequency is 35.5GHz, and the SIW parameters are determined as follows: for each parameter: $a = 5.6\ mm$, $b = 2.54\ mm$, $d = 0.3\ mm$, $p = 0.5\ mm$. Therefore, the equivalent wavelength λ_g transmitted in the SIW is about 6.75 mm [6].

B. SLOT ANTENNA DESIGN

According to the antenna installation requirements, the main beam needs to be biased to the load, so the slot spacing is greater than $\lambda_g/2$. The calculation formula of the main beam declination is shown in equation (3), where λ is the wavelength transmitted in free space, λ_g is the wavelength transmitted in SIW, and S is the slot spacing [2]. According to the main beam declination $\theta \approx 26°$, the slot spacing is about 5.2 mm.

$$\theta = \arcsin\left(\frac{\lambda}{\lambda_g} - \frac{\lambda}{2S}\right) \tag{3}$$

When the standard metallic hollow waveguide WR28 (a= 7.112mm, b=3.556mm, see the standard: *GB11450.2-1989*) is adopted, the wavelength transmitted in the corresponding waveguide is 10.51mm. At the same beam declination $\theta \approx 26°$, the slot spacing is about 11.6 mm. Therefore, the length of the slot array of the SIW structure is only 44.8% of the length of the metal waveguide at the same number of slots. In other words, in the case of the same declination, there are 13 slots in the SIW structure, and only 5 slots in

the standard hollow waveguide. Thus, the SIW structure has significant advantages in that the antenna size is small.

The SLL is the most important parameter of the longitudinal slot antenna, which requires amplitude synthesis for each radiating slot. For the SIW longitudinal slot, the magnitude of radiation intensity was determined by the offset of slot from the waveguide center. The larger the offset is, the greater the radiation intensity (conductance) is. Therefore, only by knowing the relationship between the offset and the radiant energy can the synthesis of the pattern be performed. In the past few decades, many theoretical and numerical calculation methods for slot array antennas have been proposed [2]–[5]. To accurately calculate the slot parameters, the internal mutual coupling and external mutual coupling between the slots must be taken into account. In [4], by simulating a slot antenna with the same slot offset, the relationship between slot offset and conductance can be solved. The number of slots must be >15, so the number of slots is set to 15. Therefore, all mutual coupling between the slots is included.

The relationship between the conductance and S-parameter of the slot array is shown in Equation (4).

$$g = 1 - q\left(\frac{|S_{21}|^2}{1-|S_{11}|^2}\right)^{\frac{1}{N}} \tag{4}$$

where S_{11} is the reflection coefficient of port 1, S_{21} is the transmission coefficient of two ports, $N=15$ is the number of slots, and q is the attenuation coefficient between two adjacent slots in SIW. The simulated transmission attenuation of SIW with a length of *78mm* is -0.25 *dB* (transmission energy is *0.944*), and the adjacent slot spacing is *5.2mm*, so q can be solved as follows:

$$q^{78/5.2} = q^{15} = 0.944 \tag{5}$$

Thus, the attenuation coefficient $q = 0.996$ can be obtained. S_{21} is required to resonate at a center frequency of *35.5 GHz*, so that a corresponding slot length can be given. Combined with HFSS simulation, the 15-slots with the same offset are simulated. The simulated S-parameters, conductance and resonant lengths are shown in Table 1.

To obtain a good radiation performance, the Taylor synthesis [2] of SLL= −25 dB was adopted. Due to the limited antenna size (<80mm), the actual antenna can only arrange 13 slots. The normalized current and conductance distribution of each slot is shown in Fig. 2. In Taylor synthesis, the current distribution of each slot is symmetric about the intermediate slot, but the conductance of each slot is asymmetrical. The reason is that in the traveling wave array, as the energy propagates in the SIW, the energy is gradually attenuated and radiated. Therefore, the slot conductance near the feed is small, and the conductance near the load is large, thus ensuring that the overall radiation is symmetrical.

According to the Fig. 2 and Table 1, the offset and the resonance length of each slot can be given. Since the mutual

TABLE 1. S-parameters, resonant conductance and resonant length against the slot offset at center frequency.

Slot offset (mm)	S_{21} (dB)	S_{11} (dB)	resonant conductance	Resonant length (mm)
0.1	-0.53	-29.6	-0.02	2.77
0.2	-1.36	-25.6	-0.044	2.78
0.3	-2.37	-26	-0.074	2.8
0.4	-3.88	-24	-0.116	2.82
0.5	-5.85	-22.5	-0.167	2.85
0.6	-8.23	-21.1	-0.226	2.87
0.7	-10.9	-19.4	-0.287	2.9
0.8	-13.6	-18.4	-0.344	2.93
0.9	-16.2	-17.5	-0.394	2.96
1	-18.5	-16.5	-0.435	2.99
1.1	-20.5	-15.8	-0.468	3.01
1.2	-22.9	-15	-0.506	3.03
1.3	-24.4	-14.7	-0.528	3.04
1.4	-27.5	-14.1	-0.57	3.04

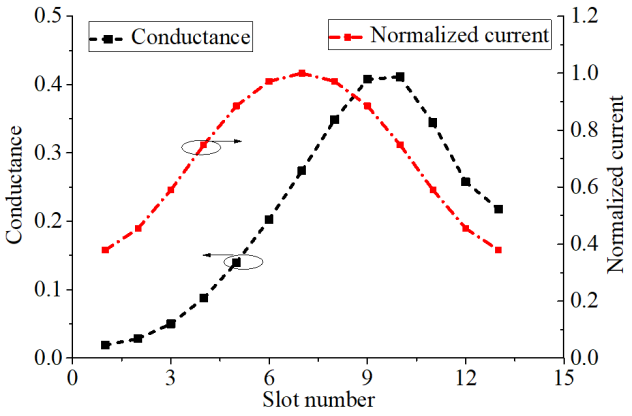

FIGURE 2. Equivalent conductance and normalized current of each slot with the number of slots N=13 (taylor synthesis of SLL = −25 dB).

coupling between the lateral and the internal slot are different, the offset of lateral slot needs to be optimally adjusted to give an optimal size. The final parameters of the slot are determined as follows (unit: mm): $L_1 = 2.78$, $L_2 = 2.78$, $L_3 = 2.79$, $L_4 = 2.81$, $L_5 = 2.84$, $L_6 = 2.89$, $L_7 = 2.91$, $L_8 = 2.96$, $L_9 = 3.02$, $L_{10} = 3.04$, $L_{11} = 3.04$, $L_{12} = 3.02$, $L_{13} = 3.02$, $Y_1 = 0.09$, $Y_2 = 0.12$, $Y_3 = 0.22$, $Y_4 = 0.33$, $Y_5 = 0.48$, $Y_6 = 0.59$, $Y_7 = 0.7$, $Y_8 = 0.88$, $Y_9 = 1.1$, $Y_{10} = 1.32$, $Y_{11} = 1.22$, $Y_{12} = 1.2$, $Y_{13} = 1.18$, $W = 0.65$, $S = 5.2$.

C. COAXIAL TO SIW CONVERSION DESIGN

Generally, the SIW is fed with a *50-ohm* microstrip line. However, for a compact design, it is fed through a *50-ohm* coaxial line similar to the metal rectangular waveguide, shown in Fig. 3. When the antenna is actually assembled, one end of the coaxial inner conductor is inserted into the SIW dielectric, and the other end is directly connected to the receiving circuit plate, as seen in Fig. 5. The coaxial line

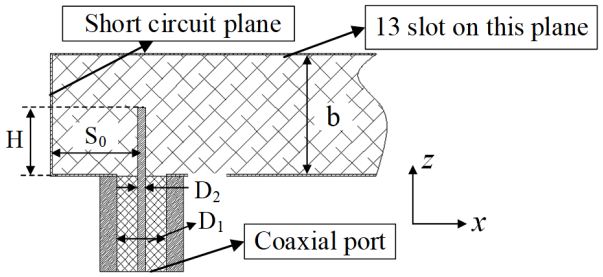

FIGURE 3. Cross-section view of the proposed antenna and the geometry of the coaxial port.

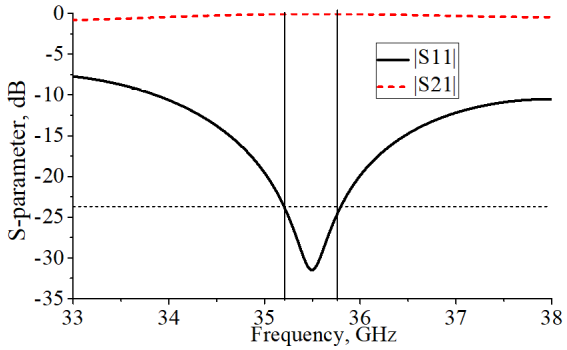

FIGURE 4. Simulated s-parameter of the coaxial to siw conversion (port 1 represents the coaxial and port 2 represents the siw).

adopts a glass insulator, and the dimensions of the coaxial outer and inner conductors are $D_1 = 1.6\ mm$, $D_2 = 0.3\ mm$, and the dielectric constant of the insulating part is *4.97*.

The design principle of coaxial line to SIW is similar to that of coaxial to metallic waveguide [23]. That is to say, the TEM mode in the coaxial line is converted into the TE_{10} mode in the metal rectangular waveguide. According to the waveguide theory, the electric field at $\lambda_g/4$ or $3\lambda_g/4$ from the short-circuit plane is the strongest, where λ_g is the wavelength transmitted in the waveguide. Therefore, the coaxial line is usually selected at these positions for maximum conversion efficiency, and $\lambda_g/4$ is selected here. The coaxial inner conductor is inserted into the middle of the narrow wall of the waveguide, that is, the length of the probe is about *b/2*. The final parameters of the coaxial conversion are determined as follows (unit: mm): $H = 1.2\ mm$, $S_0 = 1.73$. The simulated S-parameter of the coaxial to SIW conversion is shown in Fig. 4. As seen in Fig. 4, the transmission performance is particularly good within the operating frequency bandwidth.

The above three parts are combined for overall design and optimized in ANSYS High Frequency Structure Simulator (HFSS). According to the optimal design, the antenna is processed and tested to verify the accuracy of the design.

III. MEASURED RESULTS AND DISCUSSION

The photograph of the proposed antenna is pictured in Fig. 5. The antenna is set to dual port in simulation, where the coaxial port is port 1 and the matching load is port 2, as shown in Fig. 1(a). The antenna prototype is designed as a single

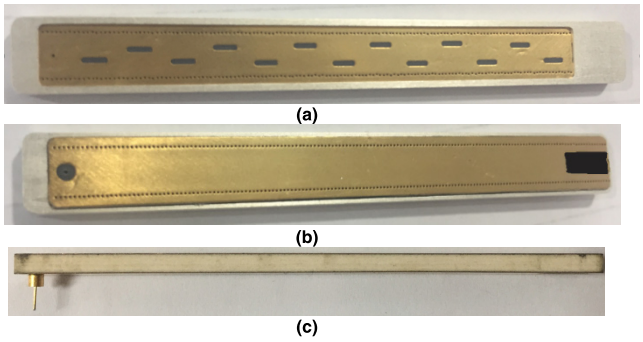

FIGURE 5. Photograph of proposed antenna. (a) Front view. (b) Back view, (c) Side view. a metal shell has been added in (a) and (b).

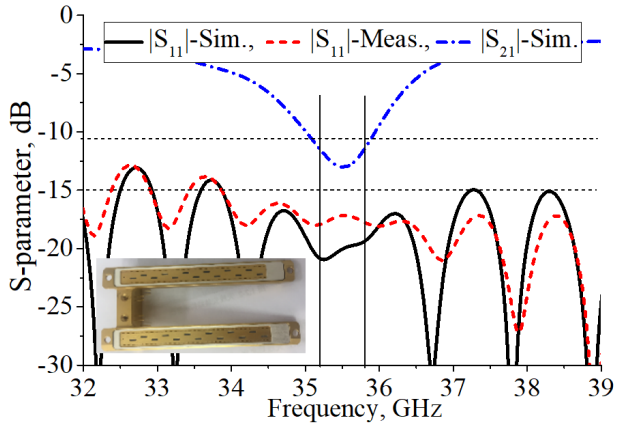

FIGURE 6. Measured and simulated S-parameter. The photo in the lower left corner is the antenna conformal on the surface of the projectile bracket.

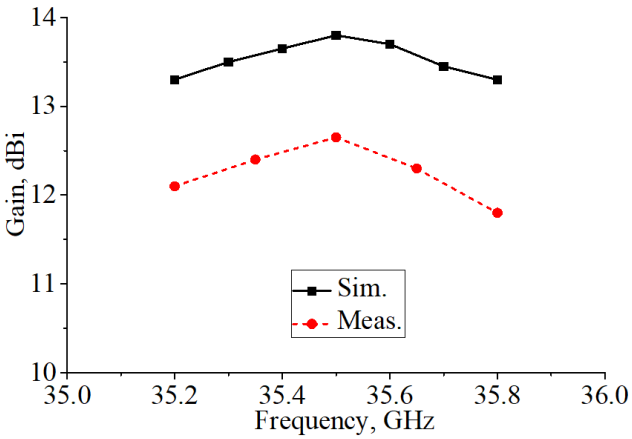

FIGURE 7. Simulated and measured gains of the proposed antenna.

port for compactness, the coaxial port is the input port, and the other end is directly connected to a matching load.

Agilent Vector network analyzer 8722ET is used to measure the reflection coefficient of the proposed antenna, and is shown in Fig. 6. The impedance bandwidth of the antenna is very wide with a reflection coefficient of below than -15dB, and the simulated and the measured results have a good agreement. Since the antenna sample is a single port, only

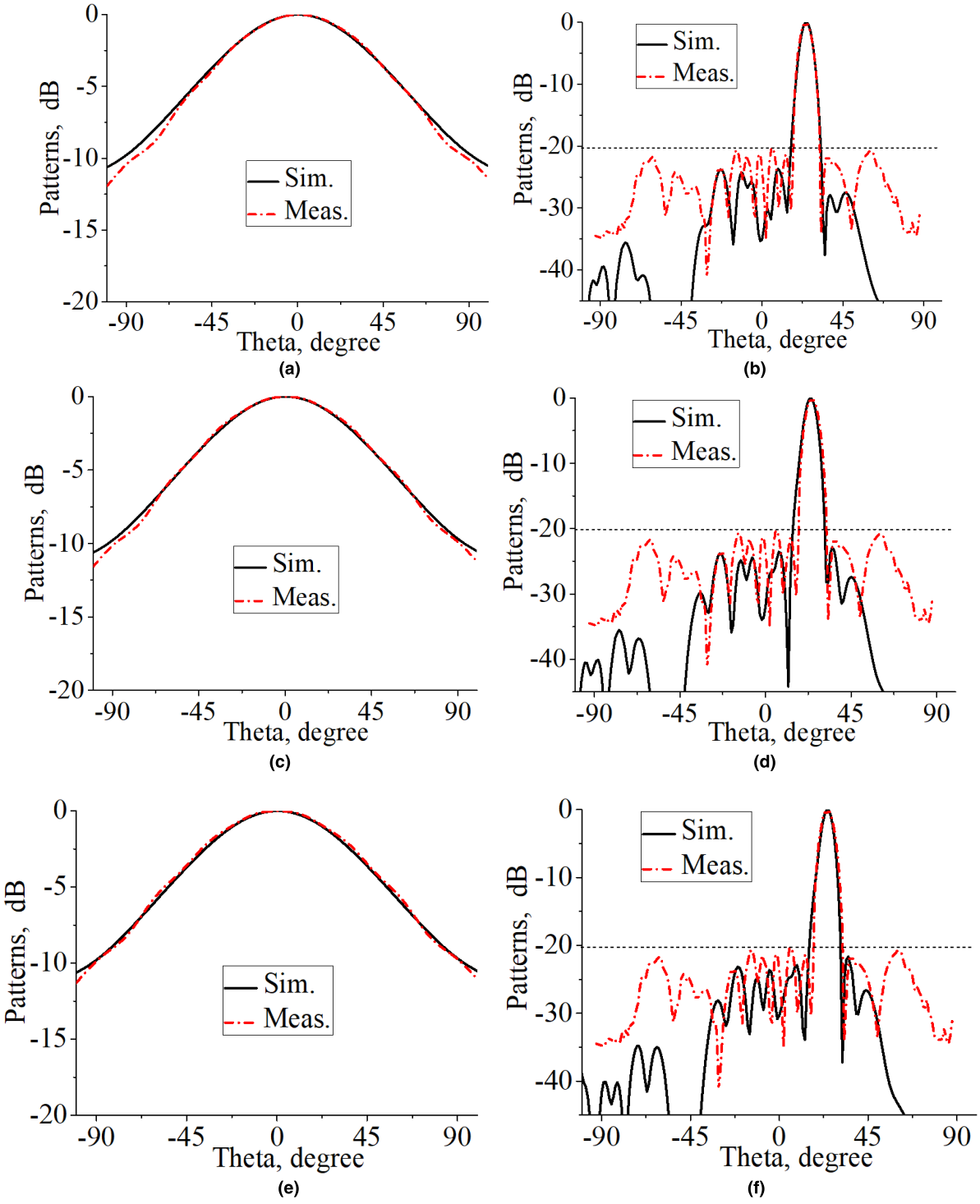

FIGURE 8. Simulated and measured radiation patterns in E-plane at frequencies of (a) 35.2GHz, (c) 35.5GHz, (e) 35.8GHz, and in H-plane at frequencies of (b) 35.2GHz, (d) 35.5GHz, and (f) 35.8GHz.

the reflection coefficient S_{11} of the port 1 can be measured, and the transmission coefficient S_{21} cannot be measured. In general, the radiation efficiency is an important parameter of the antenna. The radiation efficiency is "G/D". "G" is the gain of antenna and "D" is the directivity of antenna. The radiation efficiency can also be estimated from another method by the S_{21}. From the simulated S_{21}, the transmission coefficient is about 7% (−11.5 dB), that is, the energy absorbed by the load is 7%. Combined with simulation, the transmission loss and leakage of the SIW is less than 5.6% (−0.25 dB). Since the energy is conserved, the radiation efficiency of the antenna is greater than 87%.

TABLE 2. Units for magnetic properties simulated and measured SLL and beam declination in H-plane.

Frequency (GHz)	SLL (dB)		Beam declination (°)	
	Sim.	Meas.	Sim.	Meas.
35.2	-23.95	-20.7	26.4	26.3
35.5	-22.88	-20.1	26	25.8
35.8	-22.1	-20.6	25.7	25.4
	E-plane		H-plane	

The radiation pattern, gain, and beam declination of the prototype antenna are also measured by a far-field measurement system. The simulated and measured gains for several typical frequencies are illustrated in Fig. 7. It can be found that the measured gain is about 12.3 dB±0.5dBi, and the simulation gain is 13.5±0.3dBi, which is slightly lower than the simulated one. The deviation is mainly attributed to the dielectric loss of SIW, leakage of SIW, processing inaccuracy, and the influences of the test environment.

Fig. 8 shows the measured normalized radiation pattern at frequencies of 35.2, 35.5, and 35.8 GHz, showing a good fit compared to the simulated results. The measured 3-dB beamwidth in the H-plane are 8°, 7.8°, 7.7°, and the E-plane are 81°, 80.2°, 79.6° at 35.2, 35.5, and 35.8 GHz respectively.

The measured H-plane SLL is worse than the simulated results, which may be attributed to the deviation of the dielectric constant, the processing inaccuracy of the slots and the deviation of the measurement. The simulated and measured SLL and beam declination in the H-plane are shown in Table 2. From the comparison, the measured results are very similar to the simulated results. The measured SLL is worse than the simulated, which is caused by the gap processing deviation and the test environment.

IV. CONCLUSION

A compact large-declination longitudinal slot array antenna based on the substrate integrated waveguide (SIW) technology was represented. The design of slot antenna is combined with theoretical calculation and software simulation. The antenna was processed and measured. According to the measured results, the antenna achieved a beam declination of 26° and a SLL below −20 dB. In the case of the same declination, there are 13 slots in the SIW structure, and only 5 slots in the standard metal hollow waveguide. Compared with the conventional SIW slot array [14]–[19], [22], the proposed antenna achieves a larger off angle and a lower SLL. Therefore, the slot array antenna is very suitable for application environments where the carrier is conformal and the main beam is at a large declination.

REFERENCES

[1] G. J. He, *Principles of Air Defense Missile System Equipment*, 1st ed. Beijing, China: Publishing House Electron. Ind., 2017.
[2] S. S. Zhong, *Antenna Theory and Techniques*. Beijing, China: Publishing House Electron. Ind., 2015, Ch. 6.
[3] R. S. Elliott, *Antenna Theory and Design*, Hoboken, NJ, USA: Wiley, 2003.
[4] J. Wang, Y. Nong, Z. He. *Antenna Array Theory and Engineering Applications*, 1st ed. Beijing, China: Publishing House Electron. Ind., 2015, Ch. 9.
[5] A. Morini, T. Rozzi, and G. Venanzoni, "On the analysis of slotted waveguide arrays," *IEEE Trans. Antennas Propag.*, vol. 54, no. 7, pp. 2016–2021, Jul. 2006.
[6] D. Deslandes and K. Wu, "Accurate modeling, wave mechanisms, and design considerations of a substrate integrated waveguide," *IEEE Trans. Microw. Theory Techn.*, vol. 54, no. 6, pp. 2516–2526, Jun. 2006.
[7] F. Xu and K. Wu, "Guided-wave and leakage characteristics of substrate integrated waveguide," *IEEE Trans. Microw. Theory Techn.*, vol. 53, no. 1, pp. 66–73, Jan. 2005.
[8] C. Fan, W. W. Choi, W. Yang, W. Che, and K. W. Tam, "A low cross-polarization reflectarray antenna based on SIW slot antenna," *IEEE Antenna Wireless Propag. Lett.*, vol. 16, pp. 333–336, 2017.
[9] Z. Chen, H. Liu, J. Yu, and X. Chen, "High gain, broadband and dual-polarized substrate integrated waveguide cavity-backed slot antenna array for 60 GHz band," *IEEE Access.*, vol. 6, pp. 31012–31022, 2018.
[10] Y. Cao, Y. Cai, L. Wang, Z. Qian, and L. Zhu, "A review of substrate integrated waveguide end-fire antennas," *IEEE Access*, vol. 6, pp. 66243–66253, 2018.
[11] C. Feng, T. Shi, and L. Wang, "Novel broadband bow-tie antenna based on complementary split-ring resonators enhanced substrate-integrated waveguide," *IEEE Access*, vol. 7, pp. 12397–12404, 2019.
[12] Z. Xiao, X. Li, Z. Qi, H. and Zhu, "140-GHz TE_{340} -Mode substrate integrated cavities-fed slot antenna array in LTCC," *IEEE J. Mag.*, vol. 7, pp. 26307–26313, 2019.
[13] M. A. Maged, F. M. El-Hefnawi, H. M. Akah, A. M. El-Akhdar, and H. El-Hennawy, "Design and realization of circular polarized SIW slot array Antenna for cubesat intersatellite links," *Prog. Electromagn. Res. Lett.*, vol. 77, pp. 81–88, Dec. 2018.
[14] J. Zhu, S. Liao, S. Li, and Q. Xue, "60 GHz substrate-integrated waveguide-based monopulse slot antenna arrays," *IEEE Trans. Antennas Propag.*, vol. 66, no. 9, pp. 4860–4865, Sep. 2018.
[15] B. Liu, W. Hong, Z. Kuai, X. Yin, G. Luo, J. Chen, H. Tang, and K. Wu, "Substrate integrated waveguide (SIW) monopulse slot antenna array," *IEEE Trans. Antennas Propag.*, vol. 57, no. 1, pp. 275–279, Jan. 2009.
[16] F. Cao, D. Yang, J. Pan, D. Geng, and H. Xiao, "A compact single-layer substrate-integrated waveguide (SIW) monopulse slot antenna array," *IEEE Antenna Wireless Propag. Lett.*, vol. 16, pp. 2755–2758, 2017.
[17] Y. Wang and A. M. Avvosh, "Software-defined reconfigurable antenna using slotted substrate integrated waveguide for Ka-band satellite-on-the-move communication," in *Proc. Int. Symp. Antennas Propag. (ISAP)*, Nov. 2015, pp. 1–3.
[18] J. Zhang, B. Li, and Z. Zhou, "A substrate integrated waveguide slot antenna for 79-GHz applications," in *Proc. Int. Workshop Antenna Technol. (iWAT)*, Mar. 2018, pp. 1–3.
[19] J. Wei, Z. N. Chen, X. Qing, J. Shi, and J. Xu, "Compact substrate integrated waveguide slot antenna array with low back lobe," *IEEE Antennas Wireless Propag. Lett.*, vol. 12, pp. 999–1002, 2013.
[20] S. Mukheriee, K. V. Srivastava, and A. Biawas, "Implementation of dual-frequency longitudinal slot array antenna on substrate integrated waveguide at X-band," in *Proc. Eur. Microw. Conf.*, Oct. 2013, pp. 195–198.
[21] S. E. Hosseininejad and N. Komjani, "Optimum design of traveling-wave SIW slot array antennas," *IEEE Trans. Antennas Propag.*, vol. 61, no. 4, pp. 1971–1975, Apr. 2013.
[22] J. F. Xu, W. Hong, P. Chen, and K. Wu, "Design and implementation of low sidelobe substrate integrated waveguide longitudinal slot array antennas," *IET Microw., Antennas Propag.*, vol. 3, no. 5, pp. 790–797, Jul. 2009.
[23] D. M. Pozar, *Microwave Engineering*. Hoboken, NJ, USA: Wiley, 2018.

CHENGWEI ZHAO was born in Shandong, China, in 1986. He received the B.S. degree in physics and the M.S. degree in theoretical physics from Qufu Normal University, Shandong, in 2010 and 2013, respectively. He is currently pursuing the Ph.D. degree with Xidian University, Xi'an, China. His areas of research interests include microstrip antennas, array antenna, slot array antennas, the diagnosis of plasma, and the interaction of plasma and electromagnetic waves.

XIAOPING LI was born in Shaanxi, China, in 1961. She received the B.S., M.S., and Ph.D. degrees from Xidian University, Xi'an, China, in 1982, 1988, and 2004, respectively, where she is currently a Full Professor with the School of Aerospace Science and Technology. Her current research interests include near-space vehicle's telemetry tracking and command, and communication technology.

CHAO SUN received the B.Eng. and Ph.D. degrees in electromagnetics from Xidian University, Xi'an, China, in 2011 and 2016, respectively, where he is currently a Lecturer with the School of Aerospace Science and Technology. His research interests include miniaturization of microstrip antennas and wideband microstrip antennas.

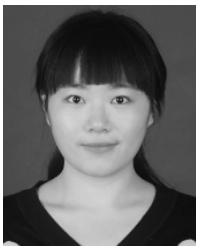

HE HUANG received the B.Eng. and Ph.D. degrees in electromagnetics from Xidian University, Xi'an, China, in 2012 and 2017, respectively, where she is currently an Associate Professor. Her research interests include dual-polarized antennas and phased-array antennas.

YANMING LIU was born in Shaanxi, China, in 1966. He received the B.S., M.S., and Ph.D. degrees from Xidian University, Xi'an, China, in 1989, 1993, and 2003, respectively, where he is currently a Full Professor with the School of Aerospace Science and Technology. His current research interest includes TT&C technology.